Cornacchia, L.; Folkard, A.; Davies, G.; Grabowski, R.C.; van de Koppel, J.; van der Wal, D.; Wharton, G.; Puijalon, S. & Bouma, T.J. (2019). Plants face the flow in V formation: A study of plant patch alignment in streams. *Limnology and Oceanography*, 64, 1087-1102

Plants face the flow in V-formation: a study of plant patch alignment in streams

Authors:

Loreta Cornacchia[1,7, a] loreta.cornacchia@nioz.nl, loreta.cornacchia@univ-lyon1.fr
Andrew Folkard[2] a.folkard@lancaster.ac.uk
Grieg Davies[3] grieg.davies@southernwater.co.uk
Robert C. Grabowski[4] r.c.grabowski@cranfield.ac.uk
Johan van de Koppel[1,7] johan.van.de.koppel@nioz.nl
Daphne van der Wal[1,8] daphne.van.der.wal@nioz.nl
Geraldene Wharton[5] g.wharton@qmul.ac.uk
Sara Puijalon[6] sara.puijalon@univ-lyon1.fr
Tjeerd J. Bouma[1,7] tjeerd.bouma@nioz.nl

Affiliations:

[1] NIOZ Royal Netherlands Institute for Sea Research, Department of Estuarine and Delta Systems, and Utrecht University, P.O. Box 140, 4400 AC Yerseke, the Netherlands.

[2] Lancaster Environment Centre, Lancaster University, Lancaster, UK

[3] Southern Water Services, Southern House, Worthing, UK

[4] Cranfield Water Science Institute, Cranfield University, Cranfield, UK

[5] School of Geography, Queen Mary University of London, London, UK

[6] Univ Lyon, Université Claude Bernard Lyon 1, CNRS, ENTPE, UMR 5023 LEHNA, F-69622, Villeurbanne, France

[7] Groningen Institute for Evolutionary Life Sciences, University of Groningen, PO Box 11103, 9700 CC Groningen, The Netherlands

[8] Faculty of Geo-Information Science and Earth Observation (ITC), University of Twente, P.O. Box 217, 7500 AE Enschede, The Netherlands

[a] Present address: UMR 5023 LEHNA, Université Lyon 1, CNRS, ENTPE, Villeurbanne Cedex, France

Corresponding author:
Loreta Cornacchia
NIOZ Royal Netherlands Institute for Sea Research
Korringaweg 7
4401 NT Yerseke
The Netherlands
email: loreta.cornacchia@nioz.nl
Tel.: +31 (0)113 577 457
Fax: +31 (0)113 573 616

Running head: Plant patch alignment in streams

Keywords: *submerged aquatic macrophytes*; *spatial patterning*; *eco-hydrodynamics; bio-physical feedbacks*

Abstract

Interactions between biological and physical processes, so-called bio-physical feedbacks, are important for landscape evolution. While these feedbacks have been quantified for isolated patches of vegetation in aquatic ecosystems, we still lack knowledge of how the location of one patch affects the occurrence of others. To test for patterns in the spatial distribution of vegetation patches in streams, we first measured the distance between *Callitriche platycarpa* patches using aerial images. Then, we measured the effects of varying patch separation distance on flow velocity, turbulence, and drag on plants in a field manipulation experiment. Lastly, we investigated whether these patterns of patch alignment developed over time following locations of reduced hydrodynamic forces, using two-year field observations of the temporal patch dynamics of *Ranunculus penicillatus* in a lowland chalk stream. Our results suggest that vegetation patches in streams organize themselves in V-like shapes to reduce drag forces, creating an optimal configuration that decreases hydrodynamic forces and may therefore encourage patch growth. Downstream patches are more frequently found at the rear and slightly overlapping the upstream patch, in locations that are partially sheltered by the established upstream vegetation while ensuring exposure to incoming flow (important for nutrient availability). Observations of macrophyte patch dynamics over time indicated that neighbouring patches tend to grow in a slightly angled line, producing a spatial pattern resembling the V-formation in migratory birds. These findings point to the general role of bio-physical interactions in shaping how organisms align themselves spatially to aero- and hydrodynamic flows at a range of scales.

Introduction

Biogeomorphic landscapes, such as rivers, mangroves and salt marshes, are characterized by strong interactions between biological and physical processes. These reciprocal interactions, also referred to as bio-physical feedbacks, are fundamental for landscape formation, adjustment, and evolution (Corenblit et al. 2007; Murray et al. 2008; Corenblit et al. 2015). By obstructing the flow, vegetation stimulates channel formation in tidal marsh landscapes (Temmerman et al. 2007; Kearney and Fagherazzi 2016). In fluvial environments, riparian and floodplain plants affect the processes and morphology of alluvial rivers (Tal and Paola 2007; Gurnell 2014). Such environments are characterized by the presence of ecosystem engineers (Jones et al. 1994; Gurnell 2014), organisms that are able to modify their habitat through their action or their own physical structure or actions. To understand these biogeomorphic systems, many studies have focused on interactions between vegetation, hydrodynamics, and sedimentation processes (Leonard and Luther 1995; Madsen et al. 2001; Bouma et al. 2007). These landscapes are often characterised by patchy vegetation, at least during the establishment phase. However, despite many plants being the keystone species in these environments, understanding of how flow modification at the patch scale may affect the processes and mechanisms controlling vegetation establishment and the hydrodynamics of these systems remains limited.

The interactions between flowing water and plants have been studied across different ecosystems, over a variety of spatial scales and vegetation configurations. Such configurations include homogeneous fields of vegetation (Kouwen and Unny 1973; Nepf and Vivoni 2000; Chen et al. 2013) as well as isolated plant patches (Sand-Jensen and Vindbœk Madsen 1992; Bouma et al. 2009; Zong and Nepf 2012). The impact of a vegetation patch on hydrodynamics and sediment dynamics is location and scale-dependent (Rietkerk and Van de Koppel 2008; van Wesenbeeck et

al. 2008; Schoelynck et al. 2012), for instance changing from reduced flow velocities within the vegetation to increased velocities around it. Many more studies have been carried out on individual patches of submerged aquatic macrophytes (for example, Sand-Jensen and Mebus, 1996; Sand-Jensen, 1998; Sukhodolov and Sukhodolova, 2009), compared to studies with multiple macrophyte stands (Cotton et al. 2006; Wharton et al. 2006; Marjoribanks et al. 2017). As patches in a landscape rarely grow in isolation but rather in mosaics (Temmerman et al. 2007; Van der Wal et al. 2008), including a pseudo-braided pattern in rivers (Dawson 1989), one patch may affect other patches by altering its local environment. The size of the gap between vegetation patches can be influenced by current velocity (Fonseca and Bell 1998) and turbulence, and has implications for physical and ecological processes (e.g. sedimentation, nutrient availability) (Folkard 2005; Folkard 2011). Recent attention has been focused on the larger-scale impact of multiple patches, and how their size and/or alignment affects flow patterns (Folkard 2005; Vandenbruwaene et al. 2011; Adhitya et al. 2014) and sediment deposition (Meire et al. 2014), and the implications for landscape adjustments and evolution (Kondziolka and Nepf 2014; De Lima et al. 2015; Gurnell and Grabowski 2016). However, knowledge is still lacking on how the location of one patch may affect the occurrence of another patch, potentially leading to optimal spatial configurations due to hydrodynamic force reduction.

Several studies have revealed the importance of facilitation, i.e. positive interactions between species that promote establishment by mediation of physical stress (Bruno et al. 2003; Callaway 2007). Thus, positive feedbacks created by one patch may extend beyond the patch itself (Bruno and Kennedy 2000), leading to a facilitative effect on the establishment or growth of other species. Such interactions between vegetation patches are likely to be relevant for plant establishment in lotic environments, where primary colonization is challenging due to forces that

act to dislodge seedlings and fragments (Riis 2008; Balke et al. 2014). However, studies of facilitation mostly focus on interactions between individuals of different species or interspecific interactions (Bruno et al. 2003; Callaway 2007). Consequently, we know relatively little about intraspecific facilitation mediated by existing vegetation patches of the same species and its effects on distribution patterns in the landscape. It is important to address this gap as intraspecific facilitation is likely to be a key process in flow-dominated systems, where currents and drag forces may impose a stress that limits growth and seedling establishment (Schutten et al. 2005; Puijalon et al. 2008; Balke et al. 2011). It is known that vegetation patches may increase flow velocity in some adjacent areas, while reducing it directly downstream of the patch (Bouma et al. 2007; Chen et al. 2012; Schoelynck et al. 2012). As a consequence, optimal spatial configurations of vegetation patches might be expected to emerge due to patterns of hydrodynamic force reduction, specifically in terms of drag force reduction.

Plant-flow interactions have been studied intensively in vegetated streams because of their ecological and geomorphological importance (Gurnell 2014; Bertoldi et al. 2015; Grabowski and Gurnell 2016), and the presence of unidirectional flow makes them an ideal model system. In this study, we investigated the spatial distribution of submerged aquatic vegetation patches and the implications of this for in-stream landscape adjustments over a two-year timescale. There were three components to the study. First, naturally occurring macrophyte patches were identified from aerial images to determine the average patch separation distances. Then, a field manipulation experiment was conducted to measure the effects of varying patch separation distance on flow velocity, turbulence, and drag on the submerged plants. We considered drag reduction as a proxy for the benefits derived by plants from their location in relation to other patches. Previous studies indicate that, on a short temporal scale, the survival and establishment of individual plants depend

on successful root development (in the order of days; Barrat-Segretain et al. (1998); Barrat-Segretain et al. (1999)) and protection from scouring or dislodgement due to currents and drag. Most of this primary colonization phase derives from drifting vegetative fragments, and rarely from seeds (Sand-Jensen et al. 1999; Riis 2008). To test whether the most frequent patch distributions corresponded to the locations with the lowest drag forces, we related patterns of drag reduction to the observed probability of patch occurrence identified from aerial images. After colonization, single shoots develop into patches on intra-annual time scales through clonal expansion (over the course of months; Cotton et al. (2006); Wharton et al. (2006)). Therefore, finally we tested whether such preferential patch distributions obtained from aerial images were supported by field observations of temporal patch dynamics in a lowland chalk stream over a period of two years.

Materials and methods

Measuring inter-patch distance from in-stream aerial images

To investigate the existence of preferential distributions of plant patches, we collected aerial images of an artificial drainage channel with natural colonization by aquatic vegetation. The channel is located along the Rhône River (France), near Serrières-de-Briord (45.8153 ° N, 5.4274 ° E). The channel, selected for its uniform cross-sectional and planform geometry allowing a focus on plant configuration, had an average channel width of 8.0 m, an average depth of 0.8 m, rarely exceeding 1.3 m, with relatively straight banks. Aerial images of the streambed were taken with a digital camera mounted on a pole at a height of c. 2 m. We identified 22 pairs of neighbouring patches for the dominant aquatic macrophyte *Callitriche platycarpa*. This species has long, flexible shoots that are pushed in a downstream direction by the flow, generating an overhanging canopy that is rooted

151 only at the upstream edge (Haslam 1978). The pairs could clearly be distinguished as separate
152 patches through the presence of an unvegetated area between their rooting parts. In these streams,
153 neighbouring patches were defined as those within 1.5 m from each other, because the influence of
154 an upstream patch can be observed for a distance equal to its length (Sand-Jensen and Mebus 1996;
155 Schoelynck et al. 2012), and 1.5 m is representative of the average length of *C. platycarpa* patches
156 (Sand-Jensen 1998). We measured the absolute longitudinal inter-patch distance (distance between
157 their upstream edges in the streamwise direction, L_d in m) and transversal inter-patch distance
158 (distance between their leftmost edges in the spanwise direction, T_d in m) between the pairs (Figure
159 1). To account for differences in absolute distances due to the variability in patch sizes, we
160 converted them into relative distances. To obtain relative longitudinal distances (L), we divided the
161 absolute distance L_d by the length of the upstream patch L_u. To obtain relative transversal distances
162 (T), we divided the absolute distance T_d by the width of the upstream patch T_u (Figure 1). The
163 frequency distributions of relative longitudinal and transversal distances were first converted into
164 probability distributions. Then, the probability distributions in the two directions were multiplied by
165 each other to obtain the probability of naturally-observed occurrences of vegetation patches for
166 each combination of L and T distances. This point grid was imported into GIS software and
167 interpolated to obtain a two-dimensional probability map of naturally-observed patch occurrence
168 (%) at different distances from an existing patch, using kriging interpolation.

169 **Quantifying the effects of inter-patch distance on flow velocity and drag using a field**
170 **manipulation experiment**

171 *Flow velocity measurements*

172 To assess the effects of different patch configurations on flow reduction and acceleration, we
173 measured the changes in flow velocity with varying patch separation distance through a field
174 manipulation. Plants were detached from existing patches, transplanted on perforated metal plates
175 and fixed through cable ties at the roots, to recreate two *C. platycarpa* patches (1.2 m in length, 0.6
176 m in width) that could be moved and arranged at different distances in the river bed. The two
177 patches were arranged into 10 different configurations, representing a combination of longitudinal
178 and transversal distances (Figure 2). The patch located upstream ("patch U") was kept fixed, while
179 the other one ("patch D") was moved downstream and/or laterally to create the configurations. The
180 two patches were partially overlapping in one configuration (T = 0.5, L = 0.46), as the leading edge
181 of patch D started at the end of the rooted area of patch U. In this case, the overhanging canopy of
182 patch U was located in the upper water layer, while the leading edge of patch D was located close
183 to the bed, which still allowed water to flow in between the two patches. The patch characteristics
184 (width, length and density) were kept constant between the fixed and mobile patches. Patch density
185 was fixed by fitting the plants into the perforated metal plates, with an array of 9408 holes per m^2.
186 The condition of the plant patches did not deteriorate during the course of the experiment, thus
187 maintaining a similar morphological function within the river.
188 Vertical profiles of flow velocity were measured with a 3D acoustic Doppler velocimeter
189 (ADV, Nortek) over 2 min at 10 Hz. Hydrodynamic profiles were measured at five vertical
190 locations of 5, 10, 20, 40 and 90% of the depth above the river bed. Around the pair of vegetation
191 patches, vertical profiles were located at distances of 0.2 m and 0.1 m respectively from the
192 upstream edges, and 0.2 m on both sides of each patch (at 0.35 m along their length), i.e. in the gap
193 between the patches. For each point measurement in the profile, mean values of the velocity
194 components u, v and w were calculated (corresponding to velocities in the x, y and z directions; m s^{-1}).
195 Depth-averaged flow velocities u (in the streamwise direction) are expressed relative to

196 incoming flow velocity, which was recorded at a fixed measurement point located 0.5 m upstream
197 of patch U.

198 *Turbulent kinetic energy*

199 To determine the effects of different patch configurations on turbulence, we measured the changes
200 in turbulent kinetic energy (TKE, $m^2\ s^{-2}$) with different patch separation distances. TKE is a
201 measure of hydrodynamic turbulence that can negatively affect plants through direct effects on their
202 growth (Jaffe and Forbes 1993). Also, by governing processes of sediment trapping and
203 resuspension (Hendriks et al. 2008), it can potentially affect plant establishment by reducing
204 sediment stability. TKE was therefore calculated for the profile located at 0.1 m from the upstream
205 edge of patch D, to investigate its potential implications for establishment. We first calculated the
206 turbulent fluctuations $u'(t) = u(t) - \overline{u}$ where $u(t)$ is the time series of flow measurements and $\overline{u}$
207 is the time-averaged velocity ($m\ s^{-1}$) in the streamwise direction at each vertical position. The
208 corresponding spanwise and vertical turbulent velocity components v' and w' were calculated in
209 the same way. For each point measurement in the profile, turbulent kinetic energy (per unit mass)
210 was then calculated as $TKE = \frac{1}{2}\left(\overline{u'^2} + \overline{v'^2} + \overline{w'^2}\right)$.

211 *Drag force measurements*

212 To investigate the benefits of different patch configurations in terms of drag reduction, we
213 measured the effects of varying patch separation distance on drag forces. Drag forces were
214 measured using a force transducer developed by the former WL Delft Hydraulics (now Deltares,
215 Delft, The Netherlands). The transducer consisted of a solid platform, carried by two steel
216 cantilever beams, with four temperature-corrected strain gauges mounted in pairs on opposite sides
217 of each of the two steel cantilevers (for details see Bouma et al. (2005)). The voltage output for the

force transducer was linearly correlated with forces up to 10 N ($r^2 = 0.99$, $p < 0.001$). During the measurements, a *C. platycarpa* plant was mounted on top of the transducer and placed into the river bed at the upstream edge of patch D. For the measurements, we selected isolated plants of 55.1 ± 5.8 cm in height and with 4 to 9 ramifications. Plants were attached to the transducer by their stem, and positioned in a natural growth position to closely represent the natural conditions. Voltage readings were collected on a data logger at a frequency of 100 Hz and expressed as the mean value for 1 min. As bending and leaning of the plant on the vegetation patch interferes with measuring the actual drag on the individual, drag measurements were also performed by removing patch D and repeating the measurement on the single plant. To allow comparisons between individuals, drag was expressed as a function of total plant surface area.

Effects of patch interactions on seasonal in-stream landscape adjustments: evidence from temporal field surveys

To test whether new vegetation occurred preferentially at certain distances and directions from initial vegetation patches, we analysed field surveys of vegetation development from a study on a chalk stream reach within the Frome-Piddle catchment (Dorset, UK) over two years (monthly from July 2008 to July 2009, and bimonthly thereafter until July 2010; for further information on the field surveys, please see Davies (2012)). The study reach was the Bere Stream (UK Grid Reference 385563, 93009), a relatively straight 30 m section with bankfull widths ranging between 7-9 m. The dominant in-channel aquatic macrophyte was water crowfoot (*Ranunculus penicillatus* subsp. *pseudofluitans*) which has highly similar patch establishment dynamics and structural traits to *Callitriche platycarpa* (rooted at the upstream part of the patch and with very flexible stems that form an overhanging canopy; Haslam 1978). Furthermore, the main factors affecting initial

establishment are determined by mechanical forces (e.g. drag, flow velocity). These forces increase the risk of plant uprooting or dislodgement and relate to plant morphological characteristics (Bal et al. 2011), rather than species characteristics such as growth rates. Thus, field observations of *Ranunculus* could be compared with the findings of the field manipulation experiments of *C. platycarpa*.

The data set from the Frome-Piddle catchment afforded a unique opportunity to assess the occurrence of new vegetation and changes in vegetation cover and spatial distribution over time. The field survey was a repeated measures design over time. During each survey, macrophyte distribution was mapped along 30 transects that were located at 1-m distance intervals along the 30-m long study reach. Along each transect, measurement points were located at 0.5 m intervals to record macrophyte presence and species. The sample size was 2150 measurement points, replicated over 19 surveys, of which six surveys were used in this study. Reach survey data were analysed using GIS software. The total station coordinates of the transect markers were used to georeference a digitised version of the reach within a GIS. The output resulted in an array of points that were spatially arranged along transect lines. Vegetation cover observed at points in the reach data set were interpolated using an Inverse Distance Weighted (IDW) interpolation method. If the predicted surface outputs from IDW differed from the substrate cover observed at any extra observation point not used in the IDW, the substrate cover observed at that point prevailed above the IDW interpolation. Separate vegetation patches were derived using the minimum bounding geometry enclosing each of the polygon outputs from IDW. Although not measured in this study, seasonal changes in macrophyte cover are generally associated with changes in vegetation biomass density (g dry weight m^{-2}). A previous study in the Bere Stream found that *Ranunculus* density was lowest during winter (January, about 100 g DW m^{-2}) and peaked during the summer months (May – July), when it reached about 400 g DW m^{-2} (Dawson 1976).

We tested the hypothesis that directions of growth of new patches compared to existing patches during the survey period show preferential directions for plant growth, instead of being uniformly distributed in all directions. Therefore, six replicate surveys over three different periods were selected over the two years (December 2008 – July 2009, September 2009 – January 2010, January 2010 – July 2010) because a net increase in *Ranunculus* cover was measured within each of them, allowing the phase of new macrophyte patch colonization to be captured. The shortest distance and direction (angle) between each new vegetation patch and the closest existing patch at the beginning of each survey period were calculated using the 'Near' tool in ArcMap 10.4.

Statistical analyses

In the aerial photography, 22 replicate pairs of patches were considered. A chi-squared test was used to test for significant differences in the frequency of observed longitudinal and transversal distances between vegetation patches. In the field experiment, the statistical design was a fully factorial design with transversal and longitudinal distances as the main factors, comprising ten different configurations (treatments) each measured once. Regression analysis was used to test the effects of varying longitudinal and transversal distances on depth-averaged and near-bed (5 and 10% of depth above the river bed) flow velocities in four different positions (between the patches, at the upstream edge of patch D, next to patch U, next to patch D), and on turbulent kinetic energy at the upstream edge of patch D. We tested whether relative flow velocities would increase linearly with increasing inter-patch distances, or follow a quadratic relationship which might be expected if relative flow velocities first increase until a maximum at intermediate distances, and then decrease to 1 as they become equal to incoming flow velocity. In the latter case, patches become far enough apart so that they cease to interact. Hence, we fitted both linear and quadratic models using single (L or T distances) and multiple (L and T distances) predictor variables. We then used Akaike's

Information Criterion to compare the adequacy of the candidate models, and selected the model with the lowest AIC score (Akaike 1998). Regression analysis was used to test for the relationship between flow velocities and drag forces on *C. platycarpa* in the field flume experiment. Ordinary Least Square (OLS) regression was used for spatial regression between the experimental drag measured around a vegetation patch, and the probability of naturally-observed patch occurrence. The latter was first log-transformed (natural log of original value + 0.5) due to its skewed distribution. A chi-squared test was used to test for significant differences in angle of growth compared to a uniform distribution in all directions. A paired t-test was used to compare drag forces measured on single plants to drag on plants located at the upstream edge of a vegetation patch.

Results

Observed inter-patch distances between pairs of macrophytes

The analysis of aerial photographs from the Rhône River study reach revealed that naturally-occurring *C. platycarpa* stands display a non-random distribution relative to neighbouring patches (Figure 1). We observed that the leading edge of the downstream patch was most frequently located between one third and halfway along the length of the upstream patch (i.e., L = 0.3 – 0.5) (χ^2_8 = 20.54, p = 0.008). This longitudinal separation distance was relatively constant, regardless of the size and shape of the patches we analysed (width/length ratios ranged from 0.25 to 0.83). In the transversal direction, the downstream patch was most frequently located at 80% of the width of the upstream patch from the latter's lateral edge (i.e. T = 0.8), hence partially overlapping with, and sheltered by, the overhanging canopy of the patch ahead (χ^2_6 = 14.90, p = 0.021).

Effects of inter-patch distance on flow velocity and turbulence

Measurements of the hydrodynamic effects of different patch configurations in the Rhône River study reach showed that depth-averaged flow velocity and turbulence patterns were strongly affected by the distance between patches. In between the patches, flow velocity was strongly reduced when the patches were partly overlapping (i.e. for T = 0.5 and L = 0.46), but it increased when a clear separation developed between patches and flow was constricted. We found a significant linear relationship between flow velocities in between the patches and the relative transversal (T, spanwise) distance between the patches ($F_{1, 8} = 31.45$, $r^2 = 0.79$, $p < 0.001$; Figure 3a – c; Table 1). When the patches were close together, with no more than a 5 cm gap ($T \leq 1.08$), flow velocities between them were reduced and the pair tended to behave more like a single patch. However, flow velocity accelerated when the gap between the patches, and therefore T, increased. In particular, at T = 1.58, flow velocities between the two patches were higher than incoming velocities due to flow constriction (Figure 3b).

We found that turbulence was minimized at intermediate distances along the length of an upstream patch, while it increased both when the patches were next to each other and when one was immediately downstream of the other. Turbulent kinetic energy upstream of the patch was significantly related to relative longitudinal distance L through a quadratic relationship ($F_{2, 7} = 5.719$, $r^2 = 0.62$, $p = 0.03$), the highest TKE occurred when patches were located next to each other (for L = 0; Figure 3d – f). From L=0, TKE decreased with increased relative longitudinal distance until a minimum at L = 0.66, after which it increased again for L > 0.66 as it entered the high TKE region in the wake of the upstream patch. This minimum TKE at L = 0.66 seems to be the point at which there was an optimal combination of sheltering from the oncoming flow by the upstream patch (which increased with L), and minimization of the high TKE region in the wake of the

upstream patch (which decreased with L). For the mean flow velocities upstream of patch D, results of single and multiple regression showed no significant relationship with T and L distances (Table 1).

Areas of weakest flow deflection (i.e. reduced hydrodynamic forces) were found around the upstream patch at intermediate longitudinal distances and, in particular, when the two patches were partly overlapping. However, flow deflection increased both when the patches were next to each other and when one was immediately downstream of the other. A significant non-linear (quadratic) relationship was found between flow velocities next to patch U and both relative transversal (T) and relative longitudinal (L) distances ($F_{4, 5} = 7.931$, $r^2 = 0.90$, $p = 0.03$; Figure 3g – i; Table 1). As L increased, flow velocity first decreased for intermediate distances (between 0.16 and 0.58), due to weaker flow redirection around the patch. Then, it increased again to become equal to the incoming flow velocity, following a quadratic relationship. As T increased, and therefore the gap between the patches increased, the flow velocity increased until it was equal to the incoming flow velocity for $T \geq 1.5$. However, flow velocities next to patch D showed no significant relationship with relative transversal (T) and longitudinal (L) distances (Table 1).

Testing the relationship between patch distance and near-bed flow velocities revealed no significant relationship between patch distances and velocities at 5% of the depth above the river bed (Supporting Information, Table S1). A significant quadratic relationship between flow velocities in between the patches and both relative transversal (T) and relative longitudinal (L) distances was confirmed for flow measurements at 10% of the depth (Supporting Information, Table S2).

Effects of inter-patch distances on drag forces

Existing vegetation patches appeared to create sheltered areas where drag was minimized, and new patches were more likely to occur in these locations. Measurements of the drag force derived from a plant's particular location around an existing vegetation patch revealed a significant relationship between flow velocity and drag force per unit surface area on *C. platycarpa* individuals ($r^2 = 0.92$, $p = 0.0001$; Figure 4a). As our field drag force measurements were in the same order of magnitude as measurements performed on the same species in a laboratory flume (Puijalon et al. 2011), we assert that the field set-up provided comparable and accurate measurements. Drag forces ranged from 0.19 to 4.63 N m^{-2}, due to the flow modification by the vegetation patch, with lowest drag forces right along the lateral edge of the patch, at ≥ 0.55 m from the upstream edge. This distance along the length of the patch corresponded to the end of the rooted area and the start of the floating canopy, with the downstream patch forming an angle of 28° relative to the upstream patch. Plotting the drag in an interpolated spatial grid around a patch shows that the most frequent locations of neighbouring patches based on our field observations correspond to positions with intermediate to low drag forces (Figure 4b and d). Furthermore, the probability of observed patch occurrence in a certain position is inversely related to the observed drag force in that position (ordinary least squares spatial regression, $r^2 = 0.28$, $p < 0.0001$, Figure 4c).

Comparison of average drag force measurements on single plants, representing the conditions of initial establishment, compared to plants located at the upstream edge of a well-established patch (n = 10 configurations) showed that *C. platycarpa* individuals experience significantly higher drag when alone (Figure 5; paired t-test, $t_{19} = -2.28$, $p = 0.03$). This observation shows that drag forces on the upstream plants are mitigated by leaning onto other plants in a patch.

Effects of patch interactions on seasonal in-stream landscape adjustments: evidence from temporal field surveys

375 Field surveys over a two year period in the Frome-Piddle catchment (UK) showed that new
376 vegetation patches occurred at specific orientations from existing vegetation patches ($\chi^2_5 = 9.20$, p =
377 0.1 for Dec. 2008 – July 2009; $\chi^2_5 = 12.80$, p = 0.025 for Sept. 2009 – Jan. 2010; $\chi^2_5 = 10.88$, p =
378 0.053 for Jan. 2010 – July 2010, and $\chi^2_5 = 24.34$, $p < 0.001$ for all survey periods together; Table 2).
379 Within each of the three time periods we analysed, the most common direction of growth was at
380 angles between 0 and 60° from existing patches (with a peak around 30°), in a downstream
381 direction towards the right bank with a second most common direction at angles between 120 and
382 180°, downstream towards the left bank (Figure 6; Table 2). The most common angles of growth
383 found through field surveys are consistent with the angle of 28° found through field measurements
384 and corresponding to a region where drag forces are the lowest (Figure 4). Overall, these
385 observations support the hypothesis that new patches occur in a slightly angled line with respect to
386 existing well-established patches, in locations with reduced hydrodynamic and drag forces (Figure
387 4).

388 The observed seasonal trends of in-stream vegetation growth and die-back were similar over
389 the two survey years in the Frome-Piddle catchment (Table 2; the corresponding changes in fine
390 sediment deposition within *Ranunculus* patches are reported in Davies, 2012). During both years,
391 *Ranunculus* reached its peak cover in the period May – July and began to decline shortly after (until
392 December), due to the seasonal dieback linked to increasing channel discharge and decreasing
393 daylengths and water temperatures. In September 2009, a particularly low *Ranunculus* cover was
394 observed (7%), likely related to the increase in autumn discharges. However, in-stream vegetation
395 started to recover from January onwards, when daylengths increased, with new *Ranunculus* patches
396 recolonizing the stream bed.

Discussion

While most studies of bio-geomorphic feedbacks have focused on isolated or already established patches, our study examined the spatial configuration of patches and quantified where plant patches occur in relation to one another. A key finding was that new vegetation patches in streams organize themselves in V-like shapes during the establishment phase to reduce hydrodynamic and drag forces. Field observations showed that patches are more likely to grow at the end of the rooted area of the upstream patch, where its floating canopy starts (i.e., between one third and halfway down the length of an upstream patch), and slightly off to its side (overlapping with part of their width). Measurements in the field revealed that these locations correspond to areas where drag is reduced, due to partial sheltering from high flow velocities and TKE by well-established vegetation patches. Field manipulations supported this hypothesis, showing that mean flow velocity is reduced by partially overlapping with upstream patches in the across-stream direction, and turbulence is minimized when growing halfway down the length of an upstream patch in the main flow direction. Flow deflection around the upstream patch is weakest when a partial V-shape is formed, suggesting that additional secondary patch growth can occur on the other side of the V. These patterns of patch alignment in formation resemble the formation adopted by migratory birds (Portugal et al. 2014), or the drag-reducing queue formations in spiny lobsters (Bill and Herrnkind 1976). This provides evidence of the role that bio-physical interactions have in shaping the way organisms position themselves spatially in landscapes, in both air- and water flow, across a range of scales.

Facilitative interactions within the landscape of a self-organized species

The positive and negative feedbacks underlying the formation of self-organized patterns have been identified for a wide range of ecosystems (Rietkerk et al. 2002; van de Koppel et al. 2005; Larsen et al. 2007). At the scale of a single patch, it is well known that a positive feedback of reduced flow

velocities within patches is linked to a negative feedback limiting lateral growth (Bouma et al. 2009; Schoelynck et al. 2012). However, while positive feedbacks are generally observed at a small scale within a patch (Rietkerk and Van de Koppel 2008), knowledge of the larger-scale facilitation of seedling or fragment establishment by a self-organized species is limited. Our study provides a first indication of establishment mechanisms operating at this larger, between-patch scale. We show how an existing vegetation patch modifies flow velocities and resulting drag forces in its surroundings thereby leading to positive or negative effects on the occurrence of other patches, operating at a distance. Facilitative interactions within the same self-organized species, and over larger scales, might therefore be an important but overlooked process determining the evolution of spatial patterns over time.

The spacing of the vegetation patches resembles the organized spatial configurations observed in other organisms. For instance, migratory birds maximize the upward motion of air from the bird ahead and reduce drag due to air resistance (Lissaman and Shollenberger 1970; Weimerskirch et al. 2001; Portugal et al. 2014), and fish schools adopt different spatial configurations that can lead to reduced energy expenditure (Ashraf et al. 2017). Our temporal observations showed preferential patch occurrence at 0 to 60° angles from existing patches, with a peak around 30°. This angle is consistent with the 28° angle at which drag on the downstream patch was minimized in the field manipulation. However, the regions of minimum drag force did not strictly correspond to the most frequent location of patch occurrence. This discrepancy could be due to the low number of drag measurement points in that location, or to processes occurring during patch development (e.g. erosion of the upstream patch front and downstream displacement of patches (Sand-Jensen and Vindbœk Madsen 1992), nutrient availability, etc.). The observed vegetation patch configurations might involve a balance between stress reduction and nutrient

availability. For submerged aquatic plants, the position immediately in the wake of another patch could seem equally or even more beneficial in terms of drag reduction. However, the V position might be a hydrodynamic optimum to maximize drag reduction while still ensuring exposure to light and delivery of nutrients by water flow. Flume experiments on nitrogen uptake showed that ammonium uptake rates for *Callitriche* increased when the patch was located at a leading edge, where it was exposed to higher mean velocity (Cornacchia et al. 2018a). Instead, *Callitriche* had very low ammonium uptake rates when it was immediately downstream of another patch and exposed to low mean velocities. This finding suggests that partial, rather than complete, sheltering by established vegetation can allow more nutrients to be delivered to the downstream patch. Similarly, in mussel beds, aggregation at high densities provides the advantage of protection from physical forces, but also increases competition for food (van de Koppel et al. 2005; De Paoli 2017). Therefore, the balance between reducing stress and maintaining resource availability might be an important factor influencing patch distributions in different self-organized systems. Further measurements of hydrodynamics and nutrient uptake, and/or numerical modelling studies are required to investigate the physical explanation for these patterns such as the V formation.

The consistency between the neighbouring patch distances observed for *Callitriche platycarpa* and *Ranunculus penicillatus* suggest that such V-shaped settlement might be typical for lotic aquatic environments. Thus, it might be a general process for submerged aquatic vegetation in running waters, at least for species with similar morphologies and experiencing comparable drag forces (Bal et al. 2011). However, vegetation distributions can be more complex than the streamlined, V-shaped patterns described here. Moderate flow velocities and uni-directional flows tend to create a streamlined patch distribution, whereas a near-homogeneous plant cover would emerge in streams with sustained periods of low flow velocities (Cornacchia et al. 2018b).

Moreover, a model accounting for interactions between neighbouring patches of emergent vegetation found that wake interactions and resulting deposition patterns influence secondary patch growth (De Lima et al. 2015), yielding complex distributions and not necessarily recognizable V-shapes. More complex patterns in vegetation growth have also been observed in a stream with a rich abundance of aquatic plant species (Cameron et al. 2013). Plant traits could also influence the occurrence of recognizable V-shaped patterns. For instance, a V pattern might not be expected for species showing high resistance to hydrodynamic forces (Puijalon et al. 2011), high root anchorage strength (Schutten et al. 2005; Gurnell et al. 2013; Liffen et al. 2013), or relying less on areas of low velocity and fine sediment deposition for their establishment and growth. Our observations were not able to provide evidence of this distribution pattern in other species, which were not as abundant in our field sites. Further studies are necessary to test if a clear dominant species is needed to achieve this configuration, and how the presence of other species might affect the patterns and spacing between patches.

The patches in our experiment were constructed on an array of 9408 holes per m^2. As a non-dimensional measure of canopy density (Nepf, 2012), *Callitriche* patches have a frontal area per bed area $ah = 0.200 \pm 0.035$ at the incoming flow velocity of 0.24 m s^{-1} (Cornacchia et al. 2018a). This density value is similar to other studies. Bouma et al. (2007) created patches with $ah = 0.64$. In Zong and Nepf (2011), ah ranged from 0.48 to 2.52. These values fall in the dense canopy regime described in Nepf (2012), corresponding to $ah > 0.1$. Therefore, the hydrodynamic patterns presented in this study can generally be expected in other ecosystems with flexible submerged species under dense canopy conditions and presenting similar patch structure (i.e. overhanging canopies).

Initial patterns control future pattern formation: implications for ecosystem resilience

Our results on the role of patchiness on vegetation distribution suggest that initial vegetation patterns determine where future patches occur. This creates patterns at multiple spatial scales: a patch-patch scale during initial establishment, which over time leads to a pseudo-braided pattern in the organization of mature patches at the reach scale, with vegetated bands separated by unvegetated channels. These patterns likely develop on two different time scales. On the scale of generally 1 to 10 days, primary colonization by individual shoots relies on successful root development (Barrat-Segretain et al. (1998); Barrat-Segretain et al. (1999)), which allows them to withstand scouring or dislodgement due to currents and drag (as in our field manipulation). After primary colonization, single shoots develop into patches through clonal growth over the course of months, based on our monitoring data and literature studies (Cotton et al. 2006; Wharton et al. 2006). Therefore, the complex self-organized patterning of stream macrophytes likely results from processes interacting at different spatial and temporal scales.

Pattern formation at multiple scales, both spatial and temporal, has also been found to increase resilience in mussel beds which are another self-organized ecosystem (Liu et al. 2014). Similar to macrophytes, mussel aggregation into clumps improves their growth and offers protection against hydrodynamic forces (Van de Koppel et al. 2008). Thus, the presence of a few initial patches can facilitate the establishment of new patches. It might promote faster recovery following disturbance events such as floods by creating a self-reinforcing state that increases the resilience of lotic ecosystems. The sheltering effect presumably strengthens as the number of patches increases, eventually developing into near-full vegetation cover (cf. Van der Wal et al. (2008) for *Spartina* tussocks growing into a fully vegetated salt marsh). In regularly disturbed ecosystems, where the hydrologic regime and flow variability are among the primary factors controlling macrophyte establishment and development (Riis and Biggs 2003), this process may be

512 crucially important for vegetation recovery (Barrat-Segretain et al. 1998; Barrat-Segretain et al.
513 1999; Riis 2008). Our study suggests the general role of bio-physical interactions in shaping how
514 organisms align themselves to hydrodynamic flows in different landscapes and across multiple
515 spatial scales.

516 ## Acknowledgments

517 This work was supported by the Research Executive Agency, through the 7th Framework
518 Programme of the European Union, Support for Training and Career Development of Researchers
519 (Marie Curie - FP7-PEOPLE-2012-ITN), which funded the Initial Training Network (ITN)
520 HYTECH 'Hydrodynamic Transport in Ecologically Critical Heterogeneous Interfaces', N.316546.
521 Data collection in the Frome-Piddle catchment, Dorset, was supported by the Natural Environment
522 Research Council (algorithm studentship awarded to Grieg Davies) and Queen Mary University of
523 London (through a College studentship awarded to Bob Grabowski).

524 # References

525 Adhitya, A., T. Bouma, A. Folkard, M. van Katwijk, D. Callaghan, H. de Iongh, and P. Herman.
526 2014. Comparison of the influence of patch-scale and meadow-scale characteristics on flow
527 within seagrass meadows: a flume study. Marine Ecology Progress Series **516:** 49-59.
528 Akaike, H. 1998. Information theory and an extension of the maximum likelihood principle, p. 199-
529 213. Selected Papers of Hirotugu Akaike. Springer.
530 Ashraf, I., H. Bradshaw, T.-T. Ha, J. Halloy, R. Godoy-Diana, and B. Thiria. 2017. Simple phalanx
531 pattern leads to energy saving in cohesive fish schooling. Proceedings of the National
532 Academy of Sciences **114:** 9599-9604.

533 Bal, K. D., T. J. Bouma, K. Buis, E. Struyf, S. Jonas, H. Backx, and P. Meire. 2011. Trade-off between
534 drag reduction and light interception of macrophytes: comparing five aquatic plants with
535 contrasting morphology. Functional Ecology **25:** 1197-1205.
536 Balke, T., T. J. Bouma, E. M. Horstman, E. L. Webb, P. L. Erftemeijer, and P. M. Herman. 2011.
537 Windows of opportunity: thresholds to mangrove seedling establishment on tidal flats.
538 Marine Ecology Progress Series **440:** 1-9.
539 Balke, T., P. M. Herman, and T. J. Bouma. 2014. Critical transitions in disturbance-driven
540 ecosystems: identifying Windows of Opportunity for recovery. Journal of Ecology **102:** 700-
541 708.
542 Barrat-Segretain, M.-H., G. Bornette, and A. Hering-Vilas-Bôas. 1998. Comparative abilities of
543 vegetative regeneration among aquatic plants growing in disturbed habitats. Aquatic Botany
544 **60:** 201-211.
545 Barrat-Segretain, M.-H., C. P. Henry, and G. Bornette. 1999. Regeneration and colonization of
546 aquatic plant fragments in relation to the disturbance frequency of their habitats. Archiv für
547 Hydrobiologie **145:** 111-127.
548 Bertoldi, W., M. Welber, A. Gurnell, L. Mao, F. Comiti, and M. Tal. 2015. Physical modelling of the
549 combined effect of vegetation and wood on river morphology. Geomorphology **246:** 178-
550 187.
551 Bill, R. G., and W. F. Herrnkind. 1976. Drag reduction by formation movement in spiny lobsters.
552 Science **193:** 1146-1148.
553 Bouma, T., M. De Vries, E. Low, G. Peralta, I. Tánczos, J. van de Koppel, and P. J. Herman. 2005.
554 Trade-offs related to ecosystem engineering: A case study on stiffness of emerging
555 macrophytes. Ecology **86:** 2187-2199.

556 Bouma, T., M. Friedrichs, B. Van Wesenbeeck, S. Temmerman, G. Graf, and P. Herman. 2009.
557 Density-dependent linkage of scale-dependent feedbacks: A flume study on the intertidal
558 macrophyte *Spartina anglica*. Oikos **118:** 260-268.
559 Bouma, T., L. Van Duren, S. Temmerman, T. Claverie, A. Blanco-Garcia, T. Ysebaert, and P. Herman.
560 2007. Spatial flow and sedimentation patterns within patches of epibenthic structures:
561 Combining field, flume and modelling experiments. Continental Shelf Research **27:** 1020-
562 1045.
563 Bruno, J. F., and C. W. Kennedy. 2000. Patch-size dependent habitat modification and facilitation on
564 New England cobble beaches by *Spartina alterniflora*. Oecologia **122:** 98-108.
565 Bruno, J. F., J. J. Stachowicz, and M. D. Bertness. 2003. Inclusion of facilitation into ecological
566 theory. Trends in Ecology & Evolution **18:** 119-125.
567 Callaway, R. M. 2007. Direct Mechanisms for Facilitation, p. 15-116. Positive Interactions and
568 Interdependence in Plant Communities. Springer Netherlands.
569 Cameron, S. M., V. I. Nikora, I. Albayrak, O. Miler, M. Stewart, and F. Siniscalchi. 2013. Interactions
570 between aquatic plants and turbulent flow: a field study using stereoscopic PIV. Journal of
571 Fluid Mechanics **732:** 345-372.
572 Chen, Z., C. Jiang, and H. Nepf. 2013. Flow adjustment at the leading edge of a submerged aquatic
573 canopy. Water Resources Research **49:** 5537-5551.
574 Chen, Z., A. Ortiz, L. Zong, and H. Nepf. 2012. The wake structure behind a porous obstruction and
575 its implications for deposition near a finite patch of emergent vegetation. Water Resources
576 Research **48:** W09517.
577 Corenblit, D., A. Baas, T. Balke, T. Bouma, F. Fromard, V. Garófano-Gómez, E. González, A. M.
578 Gurnell, B. Hortobágyi, and F. Julien. 2015. Engineer pioneer plants respond to and affect

579 geomorphic constraints similarly along water–terrestrial interfaces world-wide. Global
580 Ecology and Biogeography **24:** 1363-1376.
581 Corenblit, D., E. Tabacchi, J. Steiger, and A. M. Gurnell. 2007. Reciprocal interactions and
582 adjustments between fluvial landforms and vegetation dynamics in river corridors: a review
583 of complementary approaches. Earth-Science Reviews **84:** 56-86.
584 Cornacchia, L., S. Licci, H. Nepf, A. Folkard, D. van der Wal, J. van de Koppel, S. Puijalon, and T.
585 Bouma. 2018a. Turbulence-mediated facilitation of resource uptake in patchy stream
586 macrophytes. Limnology and Oceanography**:** doi:10.1002/lno.11070.
587 Cornacchia, L., J. Van De Koppel, D. Van Der Wal, G. Wharton, S. Puijalon, and T. J. Bouma. 2018b.
588 Landscapes of facilitation: how self-organized patchiness of aquatic macrophytes promotes
589 diversity in streams. Ecology **99:** 832-847.
590 Cotton, J., G. Wharton, J. Bass, C. Heppell, and R. Wotton. 2006. The effects of seasonal changes to
591 in-stream vegetation cover on patterns of flow and accumulation of sediment.
592 Geomorphology **77:** 320-334.
593 Davies, G. R. 2012. The transport and retention of fine sediments in seasonally vegetated lowland
594 streams. Queen Mary University of London.
595 Dawson, F. 1976. The annual production of the aquatic macrophyte *Ranunculus penicillatus* var.
596 *calcareus* (RW Butcher) C.D.K. Cook. Aquatic Botany **2:** 51-73.
597 ---. 1989. Ecology and management of water plants in lowland streams. In: Fifty-seventh annual
598 report for the year ended 31st March 1989. Ambleside, UK, Freshwater Biological
599 Association, pp. 43-60. (Annual Report, Freshwater Biological Association, Ambleside).
600 De Lima, P. H., J. G. Janzen, and H. M. Nepf. 2015. Flow patterns around two neighboring patches
601 of emergent vegetation and possible implications for deposition and vegetation growth.
602 Environmental Fluid Mechanics **15:** 881-898.

603 De Paoli, H. 2017. Restoring mussel beds: A guide on how to survive on an intertidal mudflat.
604 University of Groningen.
605 Folkard, A. M. 2005. Hydrodynamics of model *Posidonia oceanica* patches in shallow water.
606 Limnology and Oceanography **50:** 1592-1600.
607 ---. 2011. Flow regimes in gaps within stands of flexible vegetation: laboratory flume simulations.
608 Environmental Fluid Mechanics **11:** 289-306.
609 Fonseca, M. S., and S. S. Bell. 1998. Influence of physical setting on seagrass landscapes near
610 Beaufort, North Carolina, USA. Marine Ecology Progress Series**:** 109-121.
611 Grabowski, R. C., and A. Gurnell. 2016. Hydrogeomorphology—Ecology interactions in river
612 systems. River Research and Applications **32:** 139-141.
613 Gurnell, A. 2014. Plants as river system engineers. Earth Surface Processes and Landforms **39:** 4-25.
614 Gurnell, A., and R. Grabowski. 2016. Vegetation–hydrogeomorphology interactions in a low-energy,
615 human-impacted river. River Research and Applications **32:** 202-215.
616 Gurnell, A. M., M. T. O'Hare, J. M. O'Hare, P. Scarlett, and T. M. Liffen. 2013. The
617 geomorphological context and impact of the linear emergent macrophyte, Sparganium
618 erectum L.: a statistical analysis of observations from British rivers. Earth Surface Processes
619 and Landforms **38:** 1869-1880.
620 Haslam, S. M. 1978. River plants: the macrophyte vegetation of watercourses. Cambridge Univer.
621 Press. Cambridge.
622 Hendriks, I. E., T. Sintes, T. J. Bouma, and C. M. Duarte. 2008. Experimental assessment and
623 modeling evaluation of the effects of the seagrass *Posidonia oceanica* on flow and particle
624 trapping. Marine Ecology Progress Series.
625 Jaffe, M., and S. Forbes. 1993. Thigmomorphogenesis: the effect of mechanical perturbation on
626 plants. Plant Growth Regulation **12:** 313-324.

627 Jones, C. G., J. H. Lawton, and M. Shachak. 1994. Organisms as ecosystem engineers, p. 130-147.
628 Ecosystem management. Springer.
629 Kearney, W. S., and S. Fagherazzi. 2016. Salt marsh vegetation promotes efficient tidal channel
630 networks. Nature Communications **7**.
631 Kondziolka, J. M., and H. M. Nepf. 2014. Vegetation wakes and wake interaction shaping aquatic
632 landscape evolution. Limnology and Oceanography: Fluids and Environments **4:** 106-119.
633 Kouwen, N., and T. E. Unny. 1973. Flexible roughness in open channels. Journal of the Hydraulics
634 Division **99**.
635 Larsen, L. G., J. W. Harvey, and J. P. Crimaldi. 2007. A delicate balance: ecohydrological feedbacks
636 governing landscape morphology in a lotic peatland. Ecological monographs **77:** 591-614.
637 Leonard, L. A., and M. E. Luther. 1995. Flow hydrodynamics in tidal marsh canopies. Limnology
638 and Oceanography **40:** 1474-1484.
639 Liffen, T., A. Gurnell, and M. O'Hare. 2013. Profiling the below ground biomass of an emergent
640 macrophyte using an adapted ingrowth core method. Aquatic botany **110:** 97-102.
641 Lissaman, P., and C. A. Shollenberger. 1970. Formation flight of birds. Science **168:** 1003-1005.
642 Liu, Q.-X., P. M. Herman, W. M. Mooij, J. Huisman, M. Scheffer, H. Olff, and J. Van De Koppel.
643 2014. Pattern formation at multiple spatial scales drives the resilience of mussel bed
644 ecosystems. Nature Communications **5**.
645 Madsen, J. D., P. A. Chambers, W. F. James, E. W. Koch, and D. F. Westlake. 2001. The interaction
646 between water movement, sediment dynamics and submersed macrophytes. Hydrobiologia
647 **444:** 71-84.
648 Marjoribanks, T. I., R. J. Hardy, S. N. Lane, and M. J. Tancock. 2017. Patch-scale representation of
649 vegetation within hydraulic models. Earth Surface Processes and Landforms **42:** 699-710.

650 Meire, D. W., J. M. Kondziolka, and H. M. Nepf. 2014. Interaction between neighboring vegetation
651 patches: Impact on flow and deposition. Water Resources Research **50:** 3809-3825.
652 Murray, A., M. Knaapen, M. Tal, and M. Kirwan. 2008. Biomorphodynamics: Physical-biological
653 feedbacks that shape landscapes. Water Resources Research **44:** W11301.
654 Nepf, H., and E. Vivoni. 2000. Flow structure in depth-limited, vegetated flow. Journal of
655 Geophysical Research: Oceans **105:** 28547-28557.
656 Nepf, H. M. 2012. Flow and transport in regions with aquatic vegetation. Annual Review of Fluid
657 Mechanics **44:** 123-142.
658 Portugal, S. J., T. Y. Hubel, J. Fritz, S. Heese, D. Trobe, B. Voelkl, S. Hailes, A. M. Wilson, and J. R.
659 Usherwood. 2014. Upwash exploitation and downwash avoidance by flap phasing in ibis
660 formation flight. Nature **505:** 399-402.
661 Puijalon, S., T. J. Bouma, C. J. Douady, J. van Groenendael, N. P. Anten, E. Martel, and G. Bornette.
662 2011. Plant resistance to mechanical stress: evidence of an avoidance–tolerance trade-off.
663 New Phytologist **191:** 1141-1149.
664 Puijalon, S., J. P. Léna, N. Rivière, J. Y. Champagne, J. C. Rostan, and G. Bornette. 2008. Phenotypic
665 plasticity in response to mechanical stress: hydrodynamic performance and fitness of four
666 aquatic plant species. New Phytologist **177:** 907-917.
667 Rietkerk, M., M. C. Boerlijst, F. van Langevelde, R. HilleRisLambers, J. v. de Koppel, L. Kumar, H.
668 H. Prins, and A. M. de Roos. 2002. Self-organization of vegetation in arid ecosystems. The
669 American Naturalist **160:** 524-530.
670 Rietkerk, M., and J. Van de Koppel. 2008. Regular pattern formation in real ecosystems. Trends in
671 ecology & evolution **23:** 169-175.
672 Riis, T. 2008. Dispersal and colonisation of plants in lowland streams: success rates and bottlenecks.
673 Hydrobiologia **596:** 341-351.

Riis, T., and B. J. Biggs. 2003. Hydrologic and hydraulic control of macrophyte establishment and performance in streams. Limnology and oceanography **48:** 1488-1497.

Sand-Jensen, K. 1998. Influence of submerged macrophytes on sediment composition and near-bed flow in lowland streams. Freshwater Biology **39:** 663-679.

Sand-Jensen, K., and J. R. Mebus. 1996. Fine-scale patterns of water velocity within macrophyte patches in streams. Oikos **76:** 169-180.

Sand-Jensen, K., and T. Vindbœk Madsen. 1992. Patch dynamics of the stream macrophyte, *Callitriche cophocarpa*. Freshwater Biology **27:** 277-282.

Sand-Jensen, K., K. Andersen, and T. Andersen. 1999. Dynamic properties of recruitment, expansion and mortality of macrophyte patches in streams. International Review of Hydrobiology **84:** 497-508.

Schoelynck, J., T. De Groote, K. Bal, W. Vandenbruwaene, P. Meire, and S. Temmerman. 2012. Self-organised patchiness and scale-dependent bio-geomorphic feedbacks in aquatic river vegetation. Ecography **35:** 760-768.

Schutten, J., J. Dainty, and A. Davy. 2005. Root anchorage and its significance for submerged plants in shallow lakes. Journal of Ecology **93:** 556-571.

Tal, M., and C. Paola. 2007. Dynamic single-thread channels maintained by the interaction of flow and vegetation. Geology **35:** 347-350.

Temmerman, S., T. Bouma, J. Van de Koppel, D. Van der Wal, M. De Vries, and P. Herman. 2007. Vegetation causes channel erosion in a tidal landscape. Geology **35:** 631-634.

Van de Koppel, J., J. C. Gascoigne, G. Theraulaz, M. Rietkerk, W. M. Mooij, and P. M. Herman. 2008. Experimental evidence for spatial self-organization and its emergent effects in mussel bed ecosystems. Science **322:** 739-742.

van de Koppel, J., M. Rietkerk, N. Dankers, and P. M. Herman. 2005. Scale-dependent feedback and regular spatial patterns in young mussel beds. The American Naturalist **165:** E66-E77.

Van der Wal, D., A. Wielemaker-Van den Dool, and P. M. Herman. 2008. Spatial patterns, rates and mechanisms of saltmarsh cycles (Westerschelde, The Netherlands). Estuarine, Coastal and Shelf Science **76:** 357-368.

van Wesenbeeck, B. K., J. Van De Koppel, P. MJ Herman, and T. J Bouma. 2008. Does scale-dependent feedback explain spatial complexity in salt-marsh ecosystems? Oikos **117:** 152-159.

Vandenbruwaene, W., S. Temmerman, T. Bouma, P. Klaassen, M. De Vries, D. Callaghan, P. Van Steeg, F. Dekker, L. Van Duren, and E. Martini. 2011. Flow interaction with dynamic vegetation patches: Implications for biogeomorphic evolution of a tidal landscape. Journal of Geophysical Research: Earth Surface **116**.

Weimerskirch, H., J. Martin, Y. Clerquin, P. Alexandre, and S. Jiraskova. 2001. Energy saving in flight formation. Nature **413:** 697-698.

Wharton, G., J. A. Cotton, R. S. Wotton, J. A. Bass, C. M. Heppell, M. Trimmer, I. A. Sanders, and L. L. Warren. 2006. Macrophytes and suspension-feeding invertebrates modify flows and fine sediments in the Frome and Piddle catchments, Dorset (UK). Journal of Hydrology **330:** 171-184.

Zong, L., and H. Nepf. 2011. Spatial distribution of deposition within a patch of vegetation. Water Resources Research **47:** W03516.

---. 2012. Vortex development behind a finite porous obstruction in a channel. Journal of Fluid Mechanics **691:** 368-391.

719

720 **Table 1** Regression results of linear and quadratic models including single (T, L) or multiple (T and
721 L) predictor variables. Final selected models (in bold) are based on Akaike Information Criterion
722 (AIC) values.

		Linear model			*Quadratic model*		
		Predictor variables					
		T * L	**T**	**L**	**T * L**	**T**	**L**
Relative $\overline{U}$ between patches	R^2	0.82	0.79	0.00	0.87	0.81	0.06
	p-value	0.01	0.0005	0.84	0.058	0.002	0.79
	AIC	-17.64	**-19.96**	-4.06	-16.99	-19.08	-2.67
Relative $\overline{U}$ upstream of patch "D"	R^2	0.40	0.24	0.05	0.71	0.33	0.28
	p-value	0.33	0.15	0.49	0.26	0.24	0.31
	AIC	-6.22	-7.71	-5.59	-9.37	-7.05	-6.28
Relative $\overline{U}$ next to patch "U"	R^2	0.41	0.22	0.00	0.90	0.25	0.69
	p-value	0.329	0.16	0.99	0.033	0.36	0.016
	AIC	-25.53	-26.77	-24.19	**-40.09**	-25.10	-33.95
Relative $\overline{U}$ next to patch "D"	R^2	0.33	0.31	0.00	0.38	0.31	0.085
	p-value	0.45	0.09	0.95	0.76	0.26	0.73
	AIC	-22.32	-26.05	-22.29	-19.15	-24.05	-21.18
TKE upstream of patch "D"	R^2	0.31	0.00	0.27	0.76	0.07	0.62
	p-value	0.48	0.99	0.11	0.18	0.77	0.03
	AIC	-80.09	-80.31	-83.53	-86.83	-79.04	**-87.99**

723

724

Table 2 Changes in *Ranunculus* in-stream vegetation cover (%) and direction of growth of newly occurring vegetation patches with respect to the nearest existing vegetation patch (°), based on field observations in the Frome-Piddle catchment (UK), performed over three different time periods covering the annual growth cycle. Observations were of the dominant species *Ranunculus penicillatus* subsp. *pseudofluitans*.

		Dec. 2008	July 2009	Sept. 2009	Jan. 2010	July 2010	
***Ranunculus* cover (%)**		13	22	7	22	30	
Angle to nearest vegetation patch (°)		Dec. 08 – July 09		Sept. 09 – Jan. 10	Jan. 10 – July 10		**Total**
Downstream	0 – 60	5		5	6		16
	60 – 120	0		3	1		4
	120 – 180	3		2	4		9
Upstream	180 – 240	1		0	5		6
	240 – 300	1		0	0		1
	300 – 360	1		0	1		2
Total		11		10	17		38
χ^2		9.20		12.80	10.88		24.34
d.f.		5		5	5		5
p- value		0.1		0.025	0.053		< 0.001

731 **Figures**

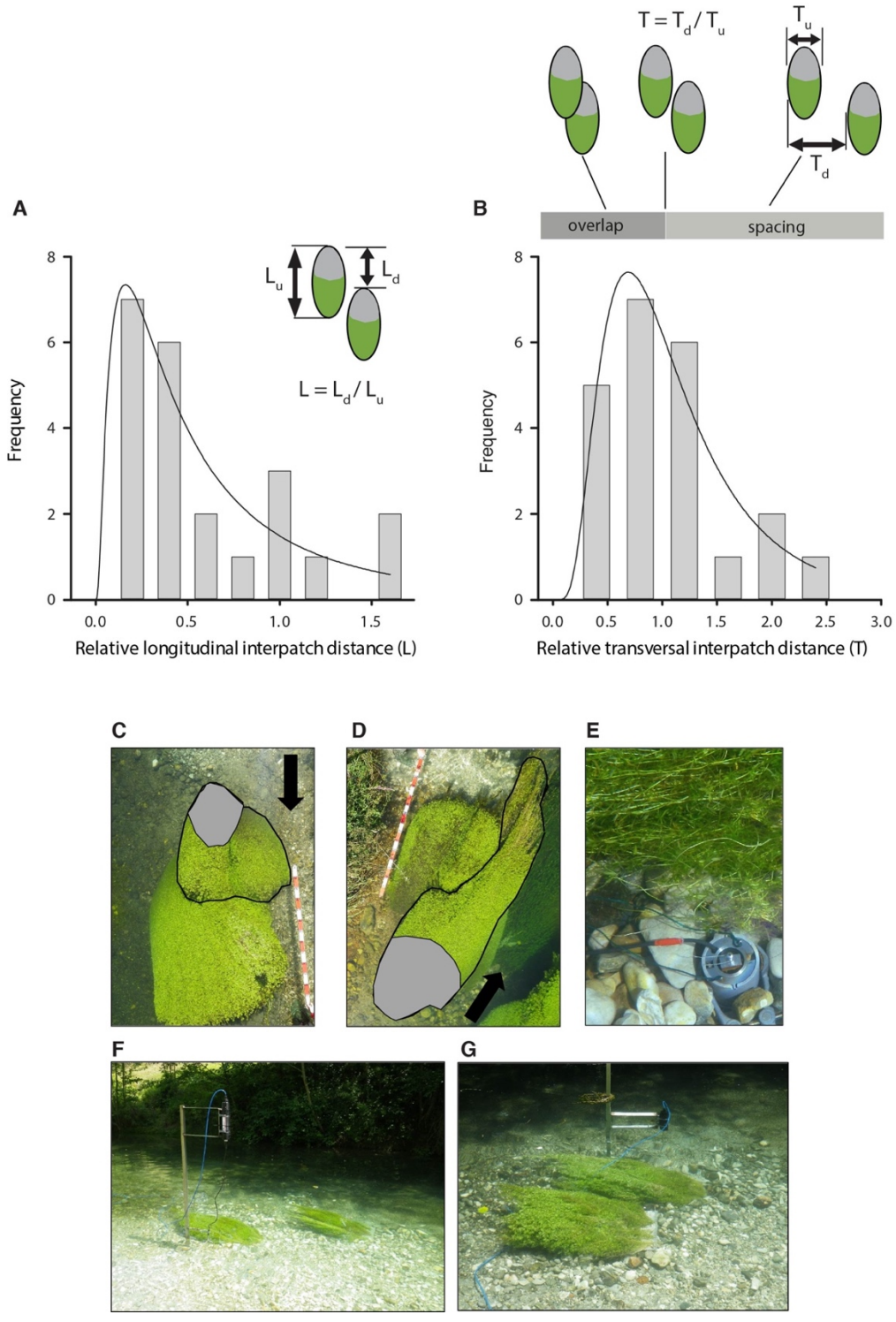

732

733 **Figure 1** Frequency distribution of A) observed relative longitudinal inter-patch distance (distance

734 between upstream edges divided by upstream patch length) and B) relative transversal interpatch

distance (transversal gap between leftmost edges divided by upstream patch width) of neighbouring patches of *Callitriche platycarpa*. The aerial pictures show macrophyte patch pairs (C, D) growing in a staggered distribution, with overlapping canopies. The canopy of the upstream patch is outlined in black. Grey areas indicate the extent of the rooted area. Arrows indicate main river flow direction. E shows the force transducer employed in the field for drag measurements on macrophytes. F and G illustrate the experimental setup in the field with the transplanted vegetation patches and ADV for flow velocity measurements.

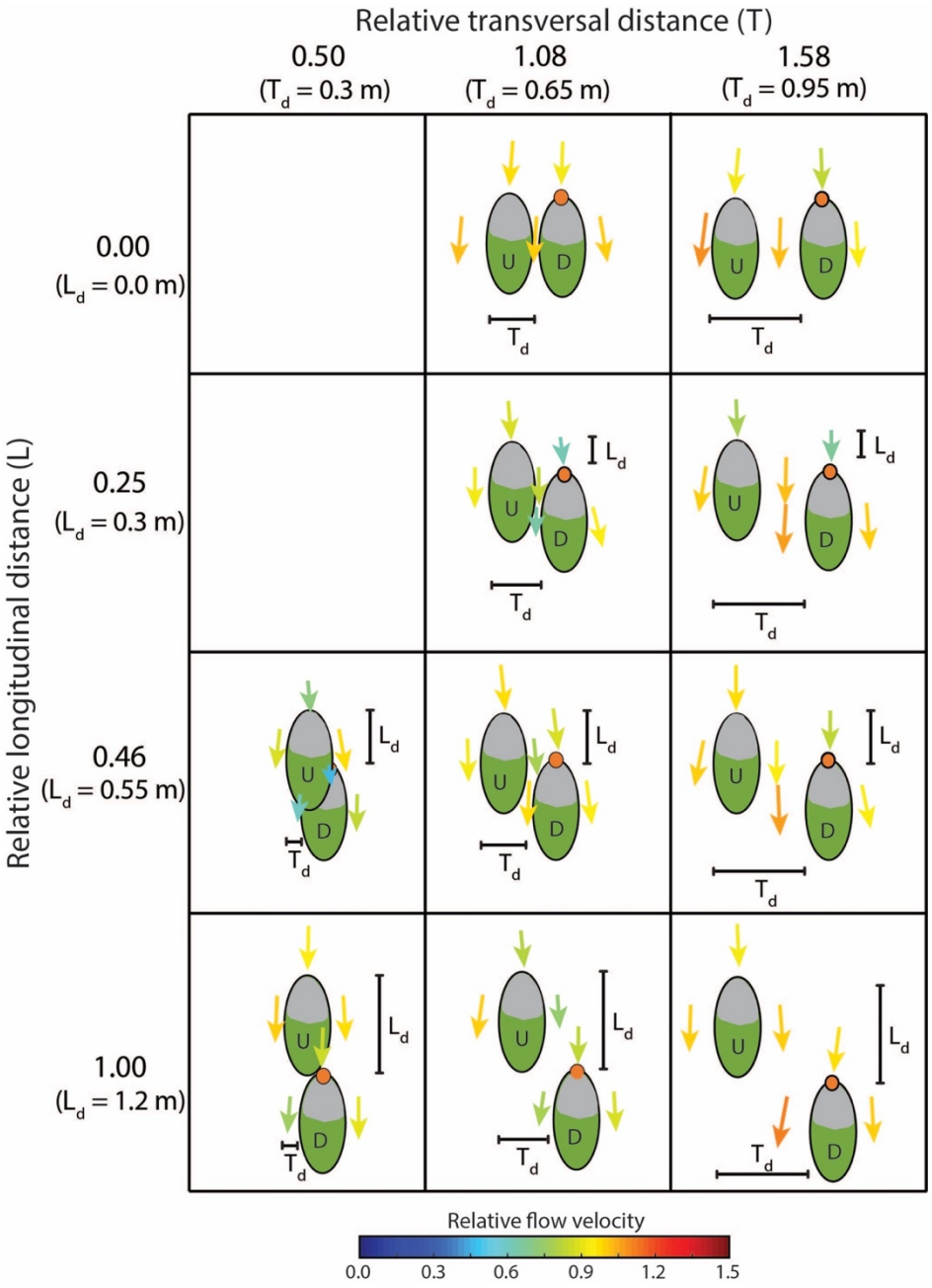

Figure 2 Overview of the ten patch configurations used in the field experiments, with indication of inter-patch distance in the longitudinal and transversal directions. L and T are relative distances; T_d and L_d are absolute distances (in m). Patch "U" was kept fixed, while patch "D" was moved downstream and/or laterally. Arrows indicate flow direction, and arrow size and colour indicate velocity magnitude relative to a measurement point located 0.5 m upstream of patch U. Grey areas indicate the extent of the rooted area. Orange dots are locations of drag measurements.

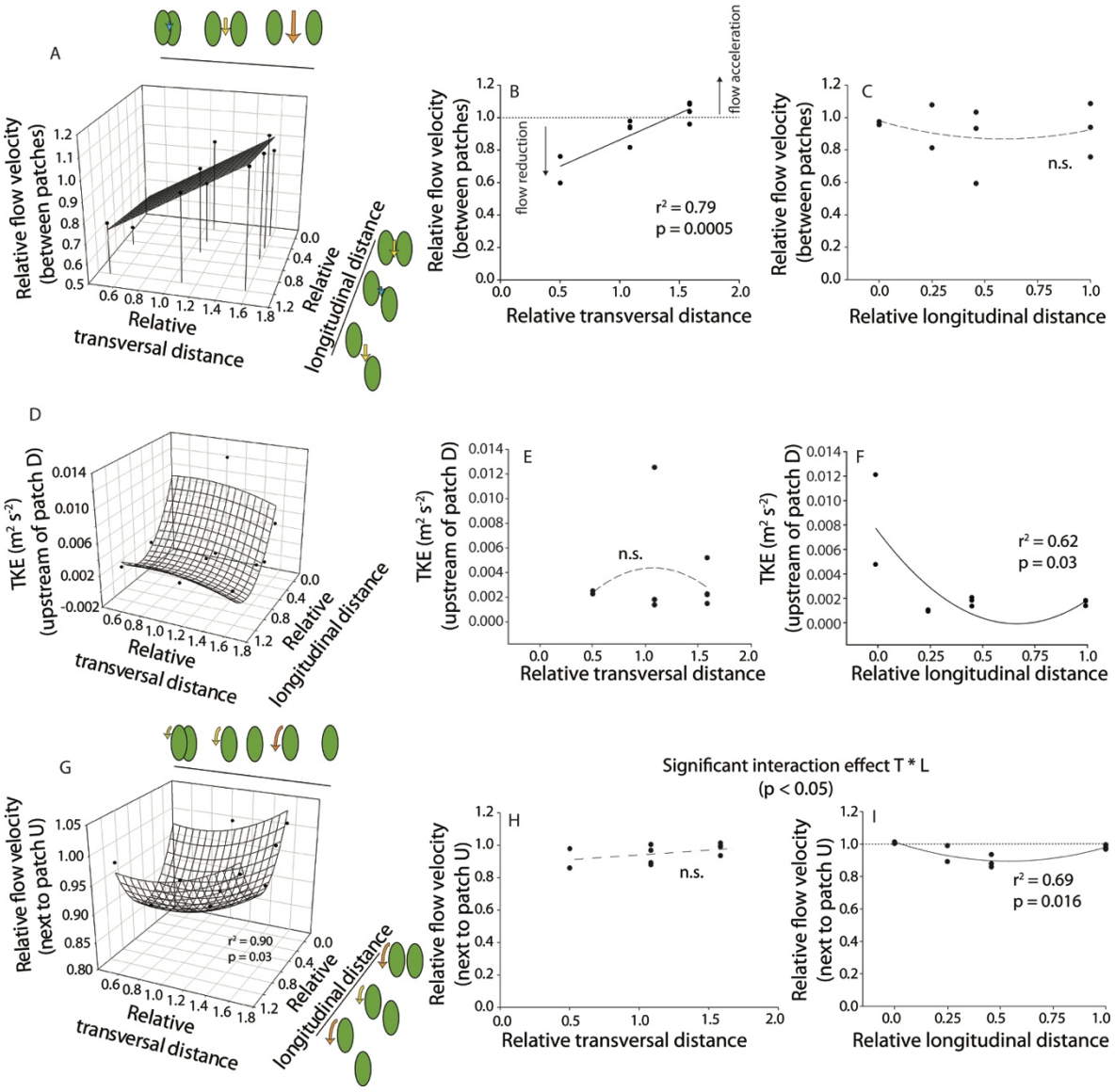

749

750 **Figure 3** Relative flow velocity measurements (flow velocity relative to incoming flow) in between
751 the patches (A, B, C) and on the side of patch U (G, H, I) for the ten configurations, showing the
752 effects of increasing relative longitudinal and transversal distances. (D, E, F) Relationship between
753 relative longitudinal and transversal distances and turbulent kinetic energy (TKE, $m^2 s^{-2}$) at the
754 upstream edge of patch D. Green ovals are illustrations of the two neighbouring patches and their
755 relative separation distances on the axes. Arrow size and colour indicate flow velocity magnitude,
756 according to the colour scale in Figure 2.

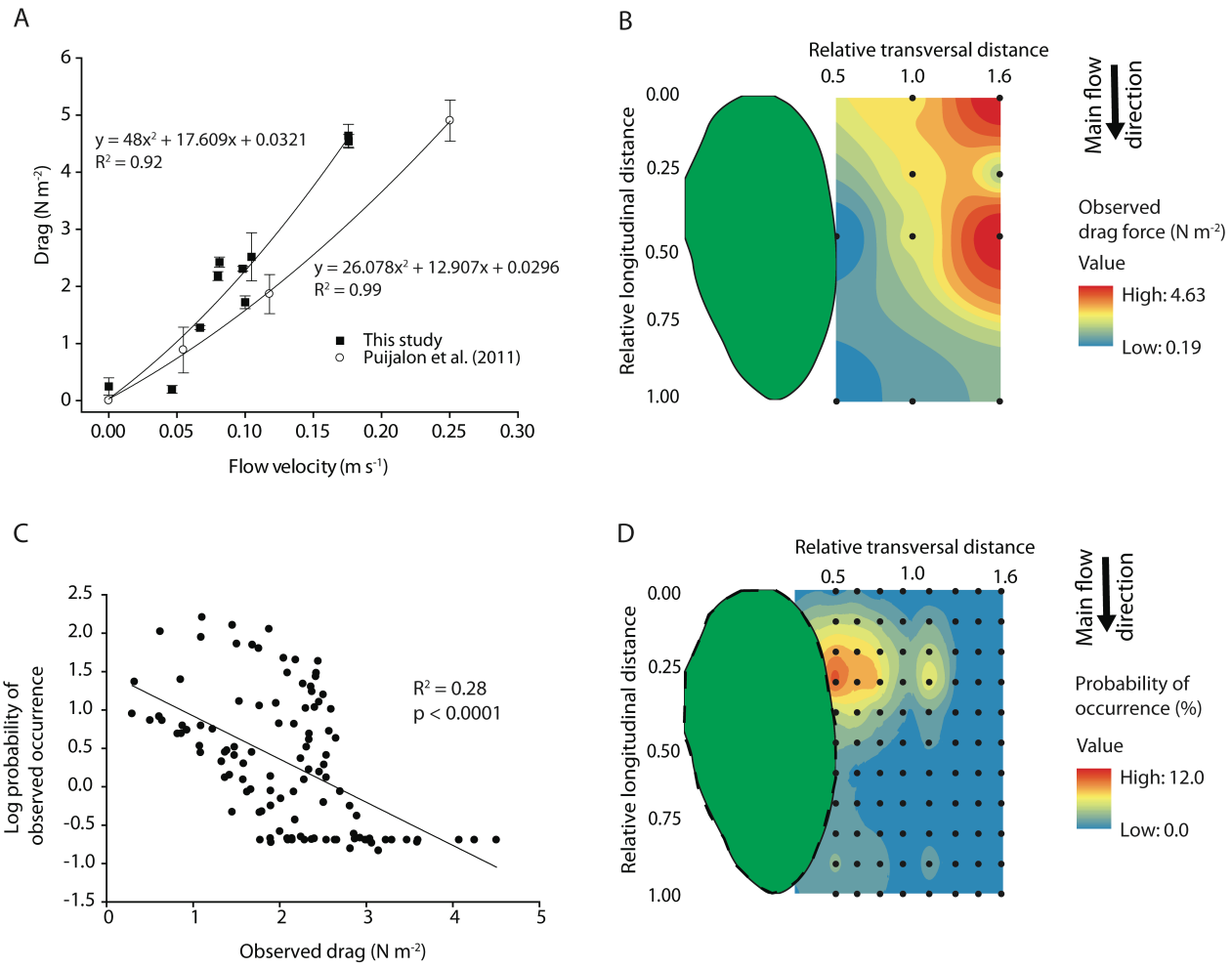

757

758 **Figure 4** (A – B) Drag forces per unit surface area on single *C. platycarpa* individuals in different
759 positions around a vegetation patch in the field flume. In A, relationship between flow velocity and
760 drag force in the field (this study) and in a laboratory flume (Puijalon et al., 2011). In B, the drag
761 measurements (black dots, same points as in A) are plotted in an interpolated spatial grid around an
762 existing vegetation patch (in green). (C – D) Probability of observed patch occurrence around an
763 existing vegetation patch. In C, spatial regression between the experimental drag in a certain
764 position around a vegetation patch, and the probability of patch occurrence in the same position. In
765 D, map of probability of patch occurrence (%), based on the combination of the observed frequency
766 distributions of relative longitudinal and transversal distances in Figure 1. Black dots indicate the

767 grid of distance observations. Note that the vegetation patch (green oval with dashed line border)
768 provides an indication of the average size of an existing patch; the actual size observed in natural
769 neighbouring patches may vary.

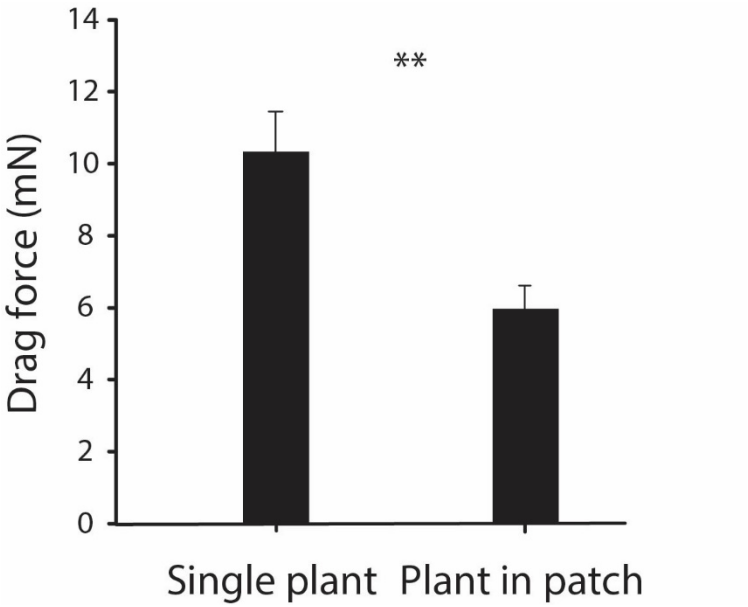

770

771 **Figure 5** Drag forces on a single plant vs. a plant located in a vegetation patch, averaged over the
772 ten vegetation configurations (paired t-test, $t_{19} = -2.2813$, $p = 0.03$). Error bars indicate standard
773 error.

774

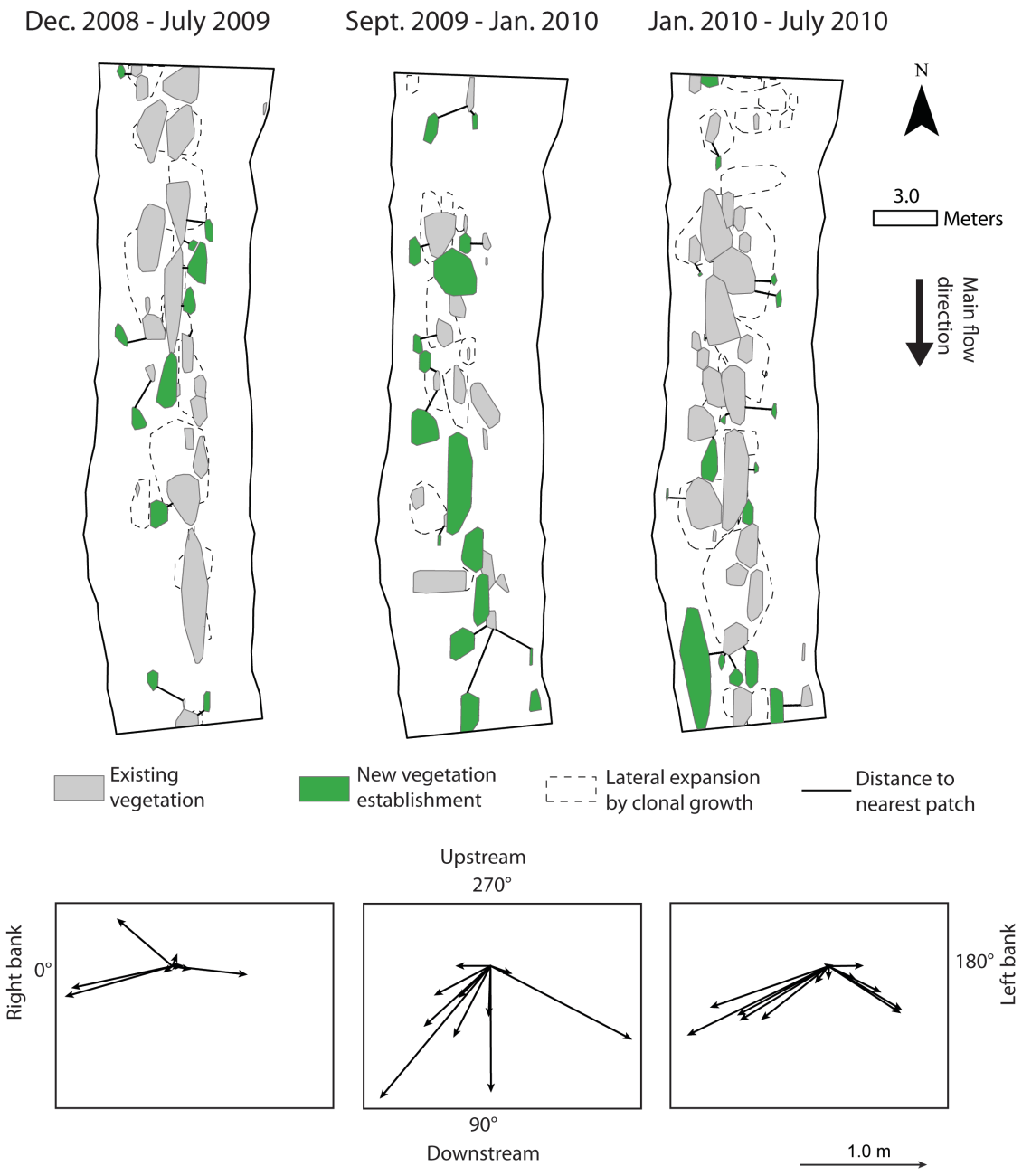

775

776 **Figure 6** *Top*: Planform representation of the distribution of in-stream macrophyte patches of

777 *Ranunculus penicillatus* subsp. *pseudofluitans*. In grey: existing vegetation patches at the start of

778 the survey period; dotted lines: lateral expansion of initial vegetation patches through clonal

779 growth; in green: new patches occurring at the end of the survey period. Black lines indicate the

780 shortest distance and direction of growth between the newly occurring vegetation and the nearest

781 existing patch. *Bottom*: distance and direction of growth (°) of new vegetation patches in each time
782 period over the stream bed.